Sensing up to 40 atm Using Pressure-Sensitive Aero-GaN

*Mircea Dragoman, Vladimir Ciobanu, Sindu Shree, Daniela Dragoman, Tudor Braniste, Simion Raevschi, Adrian Dinescu, Andrei Sarua, Yogendra K. Mishra, Nicola Pugno, Rainer Adelung, and Ion Tiginyanu**

This work reports on the fabrication and characterization of a robust pressure sensor based on aero-GaN. The ultraporous aeromaterial consists of GaN interconnected hollow micro-tetrapods with the wall thickness of about 70 nm. The inner surface of hollow micro-tetrapods contains an ultrathin film of ZnO genetically related to the sacrificial template used for epitaxial deposition of GaN. The pressure sensing measurements disclose a nearly linear dependence of the electrical conductance versus applied pressure up to 40 atm, a stable state signal being attained after an interval of about 10 s.

Aeromaterials, such as aerogels, represent three-dimensional ultra-lightweight extra-porous materials formed by randomly distributed networks of nanostructures having different sizes and shapes, such as nanowires, nanotubes, or nanosheets.[1] There is a rather limited number of materials that can be prepared as aeromaterials, but this number is continuously increasing, especially for carbon-based nanomaterials, such as carbon nanotubes, graphene, aerographite, etc.[2–5] This tremendous development of aeromaterials is related to an impressive number of applications in energy storage and conversion (e.g., supercapacitors and solar cells),[6] environmental protection (e.g., large absorption of crude oil, sensors),[7,8] biological applications (e.g., drug delivery, tissue engineering, implantable devices, and biosensing).[9] An interesting application is electromagnetic shielding where ultra-lightweight aeromaterials could replace the heavy metals used for this purpose in many industries, such as automotive and aerospace ones.[10] For many applications, pressure sensors should be robust under strongest accelerations and vibrations, additionally, for aerospace applications they need to withstand radiation, aggressive chemicals, and vacuum.

Recently, we have created a new type of aeromaterial, namely of aero-GaN or aerogalnite,[11] which can be potentially exploited for the applications mentioned above. GaN has been claimed to be a "next silicon" because of the extraordinary development of various applications of this semiconductor compound in high-frequency devices, power electronics, and optoelectronics.[12] Moreover, GaN has a large piezoelectric coefficient, useful in micro- and nano-electromechanical systems[13] and surface-acoustic-wave sensors,[14] and can be used in biological

Prof. M. Dragoman, Dr. A. Dinescu
National Research and Development Institute in Microtechnology
Str. Erou Iancu Nicolae 126A, 077190 Bucharest, Romania

V. Ciobanu, Dr. T. Braniste, Prof. I. Tiginyanu
National Center for Materials Study and Testing
Technical University of Moldova
blvd. Stefan cel Mare 168, 2004 Chisinau, Moldova
E-mail: tiginyanu@asm.md

S. Shree, Dr. Y. K. Mishra, Prof. R. Adelung
Institute for Materials Science
University of Kiel
Kaiserstrasse 2, 24143 Kiel, Germany

Prof. D. Dragoman
Physics Faculty
University of Bucharest
P.O. Box MG-11, 077125 Bucharest, Romania

The ORCID identification number(s) for the author(s) of this article can be found under https://doi.org/10.1002/pssr.201900012.

DOI: 10.1002/pssr.201900012

Dr. S. Raevschi
Department of Physics and Engineering
State University of Moldova
Alexei Mateevici str. 60, MD-2009 Chisinau, Moldova

Dr. A. Sarua
School of Physics
H.H. Wills Physics Laboratory
University of Bristol
Tyndall Avenue, BS8 1TL Bristol, UK

Prof. N. Pugno
Laboratory of Bio-Inspired and Graphene Nanomechanics
Department of Civil, Environmental and Mechanical Engineering
University of Trento
via Mesiano 77, I38123 Trento, Italy

Prof. N. Pugno
School of Engineering and Materials Science
Queen Mary University of London
Mile End Road, E1 4NS London, UK

Prof. N. Pugno
Ket Lab
Edoardo Amaldi Foundation
Via del Politecnico snc, 00133 Rome, Italy

sensors[15] thanks to its biocompatibility.[16–18] We have extended these applications demonstrating recently ultra-lightweight pressure sensors based on graphene aerogels decorated with nanocrystalline GaN films[8] and showing that an ultrathin GaN membrane with the thickness of 15 nm is acting like a memristor, analogous to a brain synapse.[19,20]

The aero-GaN could become an attractive nanomaterial for many applications. In particular, as will be shown in the following, it can be used as a pressure sensor up to 40 atm, covering the gas pressure range encountered in cars, trucks and bus tires, as well as the water pressure range in submarines, domestic house boilers, as well as aerospace applications. The aero-GaN pressure sensor is very simple and thus robust, consisting only of aero-GaN, as a pressure transducer layer, silver metallic contacts and a battery or a low-voltage DC source. **Figure 1** depicts SEM images of the initial interconnected network of the ZnO microtetrapod template (a) and the resulted aero-GaN material after the sacrificial layer of ZnO has been removed (b) and (c).

The aero-GaN material has been grown by hydride vapor phase epitaxy (HVPE) on sacrificial templates consisting of networks of interpenetrating zinc oxide tetrapods (see Figure 1 (a)). The interpenetrated ZnO network was obtained using the flame transport synthesis approach, as previously described in ref. [21]. The growth process is performed in a four-temperature-zone-heated horizontal reactor, metallic gallium, ammonia (NH_3) gas, hydrogen chloride (HCl) gas, and hydrogen (H_2) being used as source materials and carrier gases. In the source zone, GaCl was formed as a result of chemical reactions between gaseous HCl and liquid Ga at elevated temperatures. The GaCl and NH_3 gas reacted with each other in the react zone, where at the beginning the temperature was kept at 600 °C for 10 min to initiate nucleation of GaN on the surface of ZnO microtetrapods, and then increased up to 850 °C for 20 min to produce GaN layers. In the process of GaN growth, the HCl, NH_3, and H_2 flow rates were equal to 15 sml min^{-1}, 600 sml min^{-1}, and 3600 sml min^{-1}, respectively. It is to be noted that at the growth temperature of 850 °C, along with GaN deposition, simultaneous gradual decomposition and removal of the underneath ZnO template occurs. From the SEM image shown in Figure 1, it follows that the aero-GaN consists of tetrapod-shaped GaN microtubes arranged randomly, with micrometer-scale length and wall thickness around 70 nm. The degree of porosity, ε of the GaN aeromaterial exceeds 93%.

The degree of porosity was calculated using the equation $\varepsilon = (1 - \rho_a/\rho_t) \times 100\%$,[22] where ρ_a is the apparent density of the aerogel determined by the ratio of total mass ($m_{\text{aero-GaN}} = 0.06$ g) to its volume ($V_{\text{aero-GaN}} = 0.14\ cm^3$) and ρ_t represents the true density of the bulk material ($\rho_{GaN} = 6.15\ g\ cm^{-3}$).

Although the main part of the ZnO template is typically removed in the process of GaN deposition, some traces of ZnO survive on the inner surface of the aero-GaN microtubular structures. According to the statistic EDX analysis in TEM mode, the amount of Zn remaining on the inner surface of aero-GaN microtubular structures reaches values as high as 7 at%, and this amount can be reduced further down to 0.7 at% by subjecting the aero-GaN samples to a post-growth treatment in hydrogen atmosphere at 900 °C, see ref. [11] for details.

To disclose the presence of ZnO traces and their reduction during post-growth treatment in hydrogen of aero-GaN, we studied micro-Raman spectra (μRS) and micro-photoluminescence (μPL) spectra of aero-GaN samples both before and after treatment in hydrogen at 900 °C. **Figure 2**a shows typical Raman spectra taken from GaN tubular structures using a 488 nm line from Ar ion laser and a Renishaw InVia Raman system in backscattering geometry. Laser light was focused in a

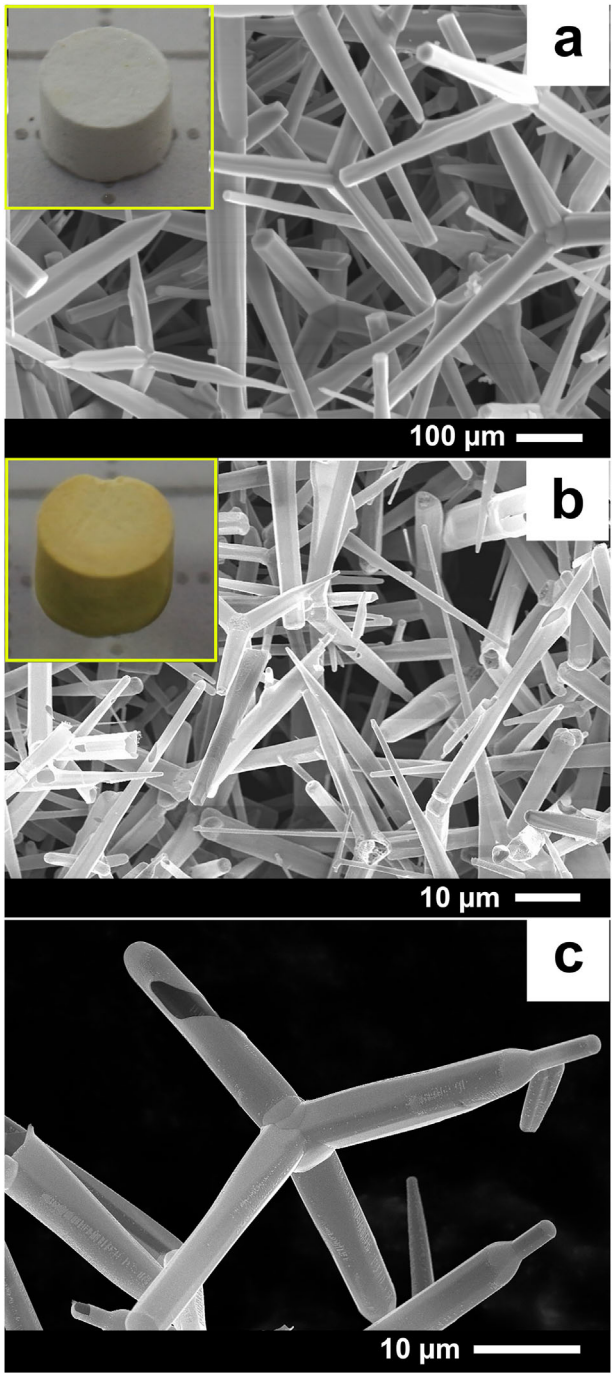

Figure 1. SEM images of interconnected network of initial ZnO (a), tubular GaN aero-material (b), and a single GaN hollow micro-tetrapod (c). The insets in (a) and (b) show the photo images of representative samples of ZnO and aero-GaN, respectively.

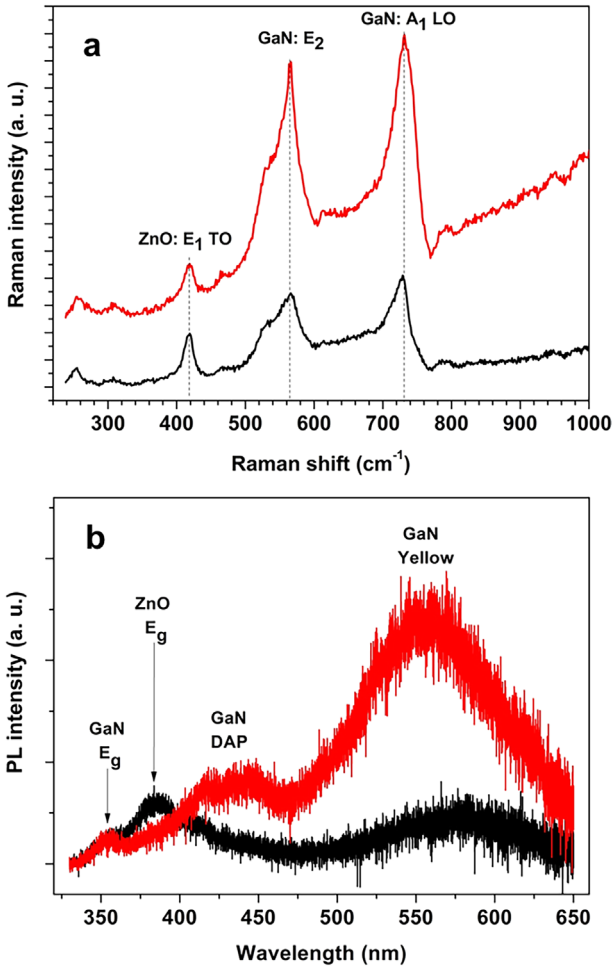

Figure 2. a) Micro-Raman scattering spectra of aero-GaN before (black curve) and after (red curve) treatment in hydrogen; dashed lines indicate position of Raman peaks in ZnO and GaN. b) Micro UV PL spectra of aero-GaN before (black curve) and after (red curve) treatment in hydrogen.

spot of about 0.6-μm diameter on an individual tubular arm of the tetrapod. The obtained Raman spectra from individual arms of tetrapods show two pronounced peaks at around 565 cm^{-1} and 732 cm^{-1}, which correspond to the E_2(high) and the A_1(LO) phonon modes of the hexagonal GaN compound. These modes are predominantly observed from (0001) c-plane of the GaN crystal, while the low frequency shoulder on the E_2(high) mode correspond to the A_1(TO) and E_1(TO) phonon frequencies, which are observed from the (1$\bar{1}$00) or equivalent crystal planes.[23] A weak Raman peak at 419 cm^{-1} corresponds to the E_1(TO) mode, or mixed quasi E_1-A_1 TO-mode, of the hexagonal ZnO, which is predominantly observed from the (1$\bar{1}$00) or equivalent planes of hexagonal crystal.[24] This is consistent with the orientation of the original ZnO tetrapods, which grow along the (0001) *c*-axis direction of ZnO, while GaN growth is predominately *c*-plane oriented. One can also observe a reduction of the ratio between the strength of GaN and ZnO modes in the Raman spectra before and after hydrogen etching. This reduction corresponds to an approximate decrease in thickness of the remaining ZnO layer after the etching by about 3.5–4 times, using ratio between corresponding Raman peak areas.

Similar results are derived from the photoluminescence spectra of the aero-GaN tertrapods using a 325-nm line from a HeCd laser and a NUV Renishaw RM-2000 spectrometer. UV μPL spectra were obtained at room temperature by focusing the laser beam on the tetrapod using ×40 NUV objective lens and minimizing incident laser power to avoid any damage due to localized heating. The resulting PL spectra in Figure 2b show that aero-GaN tetrapods exhibit primarily defect related PL bands at around 550–570 nm and 410–430 nm, with a very weak emission due to band edge related excitonic peak at around 360 nm.[25] This is consistent with the large surface area of the aero-GaN architecture and relative high defect densities in the grown GaN film, resulting in the non-radiative recombination processes and the reduction of band edge related luminescence. The observed bands around 550 nm, so called "yellow" bands, are typically related to the gallium vacancy complex point defects in the n-type GaN, while the "blue" band around 410–440 nm can be attributed to a donor-acceptor pair (DAP) type emission generated by unintentional impurity doping during growth.[25] The reduction of the remaining ZnO layer thickness after the hydrogen etching is manifested by an almost complete elimination of the ZnO band edge related emission in the UV μPL spectra (Figure 2b), usually observed at around 380 nm.[24]

The pressure sensing measurements of the aero-GaN sensor have been performed on cylindrical samples ($r = 3$ mm and $h = 5$ mm), where conductive silver paint was used for electrical contacts. A representative sample is shown in the inset of the Figure 1b. The electrical characteristics were measured using the Keithley 4200 SCS equipment with low noise amplifiers at outputs and connected to a pressure tank from Buchiglas. The aero-GaN sensor is mounted in the pressure tank which is calibrated to increase the pressure up to 40 atm by pumping pure nitrogen inside the tank. The measurements are controlled by a computer, while the temperature is preserved to be that of room temperature using a temperature monitor control which is integrated in the pressure tank. A schematic representation of the measurement setup is presented in **Figure 3**. From the *I*–*V* dependencies we have extracted the conductance, *G*, as a function of the applied pressure, *P*, as shown in **Figure 4**(a). The dependence is nonlinear, the gradient of the conductance variation with *P* decreasing with higher values of the latter parameter. Note that all measurements were made using double sweep of DC voltage and no hysteresis was observed at various sweeping rates.

The nonlinear response of the aero-GaN pressure sensor can then be attributed mostly to the variation of the contact resistance between tetrapods (i) but also to the variation of their intrinsic material resistivity with pressure (ii). From the well-known Hertz contact theory applied in the case of two crossed cylinders of equal radius (the tetrapod arms),[26] we expect a scaling between the nominal pressure/applied force *P* and contact radius *a* of the type $P \sim a^3$. Following the classical definition of the conductance $G = \sigma A L^{-1}$, with σ conductivity, A cross sectional area and *L* length of the sample, since $A \sim a^2$ we thus have $G(P) \sim \sigma(P) P^{2/3} \sim P^{\beta} P^{2/3}$, where σ is the intrinsic

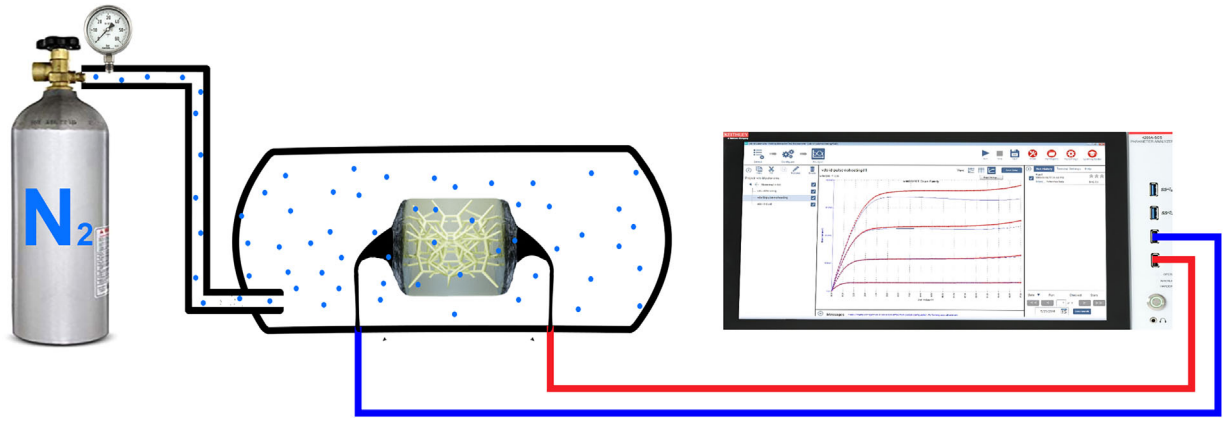

Figure 3. Schematic representation of the measurement process of aero-GaN pressure sensor.

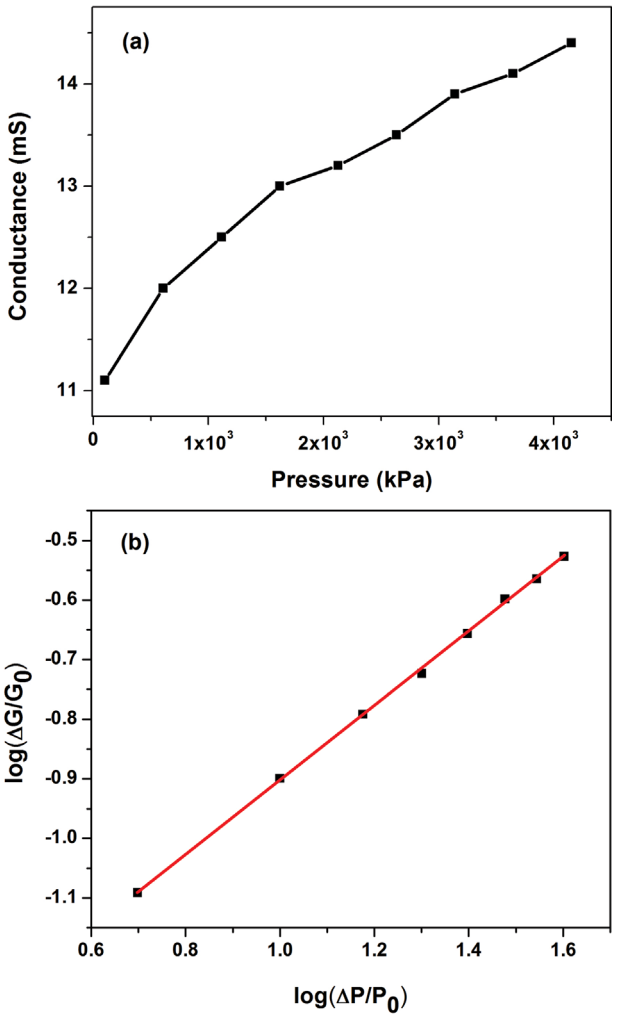

Figure 4. Conductance dependence on pressure: (a) linear and (b) double-logarithmic plots.

conductivity of the material, where the exponent 2/3 is related to the reduction of the resistance increasing the contact area (i) whereas the exponent beta is related to the intrinsic piezo-resistivity of the material (ii). Such a scaling law in the presence of non-negligible reference values (denoted with subscripts 0) becomes $(G - G_0) \sim (P - P_0)^{2/3+\beta}$. As mentioned in ref. [27], in an interconnected hollow-sphere structure, the experimental results agree with a "contact" (including also the intrinsic resistivity variation of the material) resistance-pressure dependence of the form $R_c \propto P^{-0.5}$, suggesting $\beta \cong -1/6$. Accordingly, the double logarithmic dependence of $\Delta G/G_0 = [G(P) - G_0]$, where $G_0 = G(P_0 = 1\,\text{atm})$, on $\Delta P/P_0 = (P - P_0)/P_0$ is expected to be linear, as clearly emerging from our experiment ($R^2 = 0.9995$, coefficient of determination) and as can be seen in Figure 3(b), with a slope of 0.624 thus suggesting $\beta \cong -0.043$. The dimensionless sensitivity of the pressure sensor, defined as $S = (\Delta G/G_0)/(\Delta P/P_0)$ is thus not constant and varies from 16.2×10^{-3} at low pressures (about 5 atm) to 7.4×10^{-3} at high pressures (about 40 atm). According to the derived scaling law, one could introduce a pressure-independent (thus real constant) "fractal dimensionless sensitivity" in the form of $S^* = (\Delta G/G_0)/(\Delta P/P_0)^{(2/3+\beta)}$, that from our experiments is 0.217.

The sensitivity decrease with increasing pressure is expected since an already compressed aeromaterial requires more pressure to produce the same response. No hysteresis is observed on releasing the applied pressure. Although this response is about 4.5 times lower than that of a graphene-GaN pressure sensor,[8] the current level is at least 40 times larger (see Figure 4), which makes the GaN aeromaterial sensor less sensitive to noise and easier measurable with common, portable electrical equipment. Besides, the sensitivity of the aero-GaN pressure sensor is by one order of magnitude higher than the one based on a suspended membranes.[28]

In order to investigate the temporal stability of the pressure sensor, we have applied a constant bias of −3.2 V, and observed the current over a period of about 70 s. The results, shown in **Figure 5**, reveal that, after an interval of about 10 s, the response reaches a constant plateau level. In the initial interval of 10 s, rearrangements of the random structure take place, this time interval being comparable to that required by the graphene-GaN hybrid structures[8] to attain a stable state.

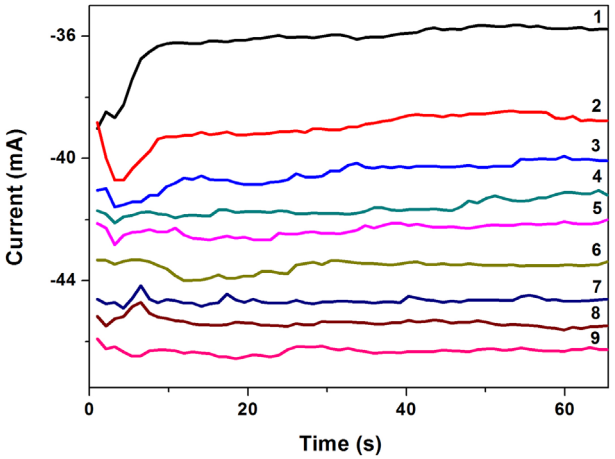

Figure 5. Time dependence of current for different applied pressures. 1 – 1 atm; 2 – 6 atm; 3 – 11 atm; 4 – 16 atm; 5 – 21 atm; 6 – 26 atm; 7 – 31 atm; 8 – 36 atm; 9 – 41 atm.

In conclusion, an ultra-lightweight pressure sensor based on aero-GaN is demonstrated. Its nondimensional sensitivity varies from 16.2×10^{-3} at low pressure (5 atm) to 7.4×10^{-3} at high pressure (40 atm). This level of sensitivity in conjunction with currents as high as tens of milliamperes makes GaN aeromaterial feasible for exploitation in portable electrical equipment. Due to the simple and robust setup, the sensor is ideal for various challenging conditions as in aerospace applications.

Acknowledgements

V.C., T.B., S.R. and I.T. acknowledge the support from the Ministry of Education, Culture and Research, Moldova, under the grants #15.817.02.29A, #15.817.02.34A, from the National Agency for Research and Development and the Science and Technology Center of Ukraine under the grant #6222 as well as from the European Commission under the grant #810652 "NanoMedTwin". N.M.P. is supported by the European Commission under the Graphene Flagship Core 2 grant no. 785219 (WP14 "Composites") and FET Proactive "Neurofibres" grant no. 732344 as well as by the Italian Ministry of Education, University and Research (MIUR) under the "Departments of Excellence" grant L.232/2016. R.A. thanks support by the DFG in the framework of SFB 1261 project A5.

Conflicts of Interest

The authors declare no conflicts of interest.

Keywords

aeromaterials, aerospace applications, gallium nitride, microtubular structures, ultra-lightweight pressure sensors

Received: January 7, 2019
Revised: February 26, 2019
Published online: March 12, 2019

[1] S. M. Jung, H. Y. Jung, M. S. Dresselhaus, Y. J. Jung, J. Kong, *Sci. Rep.* **2012**, *2*, 849.
[2] S. Chandrasekaran, P. G. Campbell, T. F. Baumann, M. A. Worsley, *J. Mater. Res.* **2017**, *32*, 4166.
[3] G. Gorgolis, C. Galiotis, *2D Mater.* **2017**, *4*, 032001.
[4] M. Mecklenburg, A. Schuchardt, Y. K. Mishra, S. Kaps, R. Adelung, A. Lotnyk, L. Kienle, K. Schulte, *Adv. Mater.* **2012**, *24*, 3486.
[5] F. Schütt, S. Signetti, H. Krüger, S. Röder, D. Smazna, S. Kaps, S. N. Gorb, Y. K. Mishra, N. M. Pugno, R. Adelung, *Nat. Commun.* **2017**, *8*, 1215.
[6] J. Mao, J. Iocozzia, J. Huang, K. Meng, Y. Lai, Z. Lin, *Energy Environ. Sci.* **2018**, *11*, 772.
[7] H. Maleki, *Chem. Eng. J.* **2016**, *300*, 98.
[8] M. Dragoman, L. Ghimpu, C. Obreja, A. Dinescu, I. Plesco, T. Braniste, I. Tiginyanu, *Nanotechnology* **2016**, *27*, 475203.
[9] H. Maleki, L. Duraes, C. A. Garcia-Gonzalez, P. del Gaudio, A. Portugal, M. Mahmoudi, *Adv. Colloid Interface Sci.* **2016**, *236*, 1.
[10] F. Meng, H. Wang, F. Huang, Y. Guo, Z. Wang, D. Hui, Z. Zhou, *Composites B, Eng.* **2018**, *137*, 260.
[11] I. Tiginyanu, T. Braniste, D. Smazna, M. Deng, F. Schütt, A. Schuchardt, M. A. Stevens-Kalceff, S. Raevschi, U. Schürmann, L. Kienle, N. M. Pugno, Y. K. Mishra, R. Adelung, *Nano Energy* **2019**, *56*, 759.
[12] F. Medjdoub, *Gallium Nitride (GaN): Physics, Devices, and Technology*, CRC Press, Boca Raton **2017**.
[13] M. Rais-Zadeh, V. J. Gokhale, A. Ansari, M. Faucher, D. Théron, Y. Cordier, L. Buchaillot, *J. Microelectromech. Syst.* **2014**, *23*, 1252.
[14] A. Muller, G. Konstantinidis, I. Giangu, G. C. Adam, A. Stefanescu, A. Stavrinidis, G. Stavrinidis, A. Kostopoulos, G. Boldeiu, A. Dinescu, *IEEE Sens. J.* **2017**, *17*, 7383.
[15] X. Li, X. Liu, *Nanoscale* **2017**, *9*, 7320.
[16] S. A. Jewett, M. S. Makowski, B. Andrews, M. J. Manfra, A. Ivanisevic, *Acta Biomater.* **2012**, *8*, 728.
[17] T. Braniste, I. Tiginyanu, T. Horvath, S. Raevschi, S. Cebotari, M. Lux, A. Haverich, A. Hilfiker, *Beilstein J. Nanotechnol.* **2016**, *7*, 1330.
[18] T. Braniste, I. Tiginyanu, T. Horvath, S. Raevschi, B. Andrée, S. Cebotari, E. C. Boyle, A. Haverich, A. Hilfiker, *Nanoscale Res. Lett.* **2017**, *12*, 486.
[19] M. Dragoman, I. Tiginyanu, D. Dragoman, T. Braniste, V. Ciobanu, *Nanotechnology* **2016**, *27*, 295204.
[20] M. Dragoman, I. Tiginyanu, D. Dragoman, A. Dinescu, T. Braniste, V. Ciobanu, *J. Appl. Phys.* **2018**, *124*, 152110.
[21] Y. K. Mishra, S. Kaps, A. Schuchardt, I. Paulowicz, X. Jin, D. Gedamu, S. Freitag, M. Claus, S. Wille, A. Kovalev, S. N. Gorb, R. Adelung, *Part. Part. Syst. Charact.* **2013**, *30*, 775.
[22] J. Wu, C. Li, D. Wang, M. Gui, *Compos. Sci. Technol.* **2003**, *63*, 569.
[23] M. Kuball, *Surf. Interface Anal.* **2001**, *31*, 987.
[24] Ü. Özgür, Y. I. Alivov, C. Liu, A. Teke, M. A. Reshchikov, S. Doğan, V. Avrutin, S. J. Cho, H. Morkoc, *J. Appl. Phys.* **2005**, *95*, 041301.
[25] M. A. Reshchikov, H. Morkoc, *J. Appl. Phys.* **2005**, *97*, 061301.
[26] H. Hertz, *Z. Reine Angew. Math.* **1882**, *92*, 156.
[27] L. Pan, A. Chortos, G. Yu, Y. Wang, S. Isaacson, R. Allen, Y. Shi, R. Dauskardt, Z. Bao, *Nat. Commun.* **2014**, *5*, 3002.
[28] A. D. Smith, F. Niklaus, A. Paussa, S. Vaziri, A. C. Fischer, M. Sterner, F. Forsberg, A. Delin, D. Esseni, P. Palestri, M. Östling, M. C. Lemme, *Nano Lett.* **2013**, *13*, 3237.